Membrane Electric Properties by Combined Patch Clamp and Fluorescence Ratio Imaging in Single Neurons

Jing Zhang,* Robert M. Davidson,# Mei-de Wei,* and Leslie M. Loew*

*Department of Physiology, University of Connecticut Health Center, Farmington, Connecticut 06030, and #Basic Science Division, New York University College of Dentistry, New York, New York 10012 USA

ABSTRACT An experimental method has been established to measure the electric properties of a cell membrane by combination of patch clamp and dual-wavelength ratio imaging of a fluorescent potentiometric dye, 1-(3-sulfonatopropyl)-4-[β[2-(di-*n*-octylamino)-6-naphthyl]vinyl]pyridinium betaine (di-8-ANEPPS). Pairs of fluorescence images from the dye-stained membrane of neuroblastoma N1E-115 cells excited at two wavelengths were initially obtained to calculate ratio images corresponding to the resting transmembrane potential. Subsequently, a whole-cell patch was established and the membrane potential clamped to levels varying from −100 to +60 mV; at each voltage, a pair of dual-wavelength images were acquired to develop a calibration of the fluorescence ratio. Using this method, the resting potentials could accurately be measured showing that the differentiated cells were 17 mV more polarized than undifferentiated cells. The combination of electrical and optical methods can also follow changes in other membrane electric properties, such as dipole potential, and thus permit a detailed analysis of the membrane electrical properties underlying the voltage regulation of ion channels.

INTRODUCTION

Voltage-gated ion channels respond to changes of the electric fields inside the cell membrane. The intramembrane potential profile is, therefore, fundamental to cell physiology, but it is difficult to measure with great certainty. The patch clamp technique is widely used to study currents through ion channels (Neher and Sakmann, 1976; Hamill et al., 1981). The whole-cell clamp configuration establishes electrical continuity between the controlling circuit and the cell interior via a tight seal between an orifice in the cell membrane and the end of a micropipette. The whole-cell clamp may be used to very precisely control and measure the transmembrane potential. However, it cannot measure variations in potential along the surface of the cell nor can it provide information on the potential profile across the membrane.

Transmembrane potentials can also be monitored with voltage-sensitive fluorescent dyes (Cohen and Salzberg, 1978; Grinvald et al., 1982; Waggoner, 1985; Loew, 1988). During the last two decades, a series of fluorescent dyes have been developed in our lab based on a putative electrochromic mechanism (Loew et al., 1979; Loew and Simpson, 1981). These dyes display rapid shifts in their spectra in response to membrane potential changes. This feature allowed us to develop a method for dual-wavelength ratiometric measurement of membrane potential (Montana et al., 1989). As in the case of dual-wavelength ratiometric measurement of intracellular ionic concentration (Tsien and Poenie, 1986), this method has advantages over single-wavelength fluorescence intensity measurements in that it can cancel out such problems as dye bleaching and uneven staining of the cell membrane. Dual-wavelength ratio imaging has also allowed us to detect variations in membrane potential along the surface of single cells and is sensitive to other important sources of intramembrane electric field, such as the dipole potential and the surface potential (Bedlack et al., 1992, 1994; Gross et al., 1994). Such regional variations in intramembrane electric fields may underlie regional variations in the behavior of voltage-gated channels (Zhang et al., 1996). However, even with ratiometric probes, spectral properties can be perturbed by a number of environmental factors; membrane-bound voltage-sensitive dyes are therefore only appropriate for measuring relative differences or changes in membrane potential.

In the present study, we have combined the whole-cell patch clamp technique with dual-wavelength ratio imaging to calibrate ratiometric dye measurements in cultured neuroblastoma N1E-115 cells. This method allows us to accurately measure the transmembrane potential of the cell without rupturing the cell membrane or disrupting the intracellular contents. The key to the approach is to carry out experimental manipulation and collect the associated ratio images before establishment of a whole-cell patch. The ratio is then calibrated against voltage applied through the patch pipette at the end of the experiment.

Received for publication 14 May 1997 and in final form 29 September 1997.

Address reprint requests to Dr. Leslie M. Loew, Department of Physiology, University of Connecticut Health Center, 263 Farmington Avenue, Farmington, CT 06030-3505. Tel.: 860-679-3568; Fax: 860-679-1269; E-mail: les@volt.uchc.edu.

0006-3495/98/01/48/06 $2.00

MATERIALS AND METHODS

Cell preparation

N1E-115 mouse neuroblastoma cells were grown at 37°C in Dulbecco's modified Eagle's medium (DMEM) supplemented with 10% fetal bovine serum. After several passages, these undifferentiated cells (usually round with no neurites) were seeded on a clean and uncoated glass coverslip and kept in the same medium before use. For some experiments, the seeded

cells were further treated with DMEM but supplemented with 1% dimethylsulfoxide (DMSO), and the fetal bovine serum was reduced to 0.5%. This treatment, given 2–5 days before use of the coverslips, induced the cells to differentiate and send out neurites. Each coverslip was washed in Earle's balanced salt solution (EBSS) buffered with 20 mM HEPES (pH 7.35) and then incubated for 20 min at 10°C in the buffered EBSS containing 1-(3-sulfonatopropyl)-4-[β[2-(di-*n*-octylamino)-6-naphthyl]vinyl]pyridinium betaine (di-8-ANEPPS; 0.5–1 μM) and Pluronic F-127 (BASF, Wyandotte, MI) (PF-127; 0.05%). Di-8-ANEPPS was prepared according to the method of Hassner et al. (1984) but is also available commercially (Molecular Probes, Eugene, OR). After the staining solution was washed away, the coverslip was mounted on the microscope chamber and maintained in the buffered EBSS solution during the experiment.

Dual-wavelength ratio imaging

Stained cells were mounted on an inverted microscope (Axiovert 135 TV, Carl Zeiss, Oberkochen, Germany) and viewed with an oil objective (Plan-apochromat 63X/1.40, Carl Zeiss). An additional magnification of $\times$2.5 was used when fluorescent images were taken. Fluorescent image pairs of single cells with the excitation at 440 and 530 nm (30-nm bandpass) were acquired (565-nm dichroic mirror and emission of $>$570 nm) using a cooled CCD camera (model CH250, Photometrics, Tucson, AZ). To diminish the vibration of the stage caused by the movement of the excitation source shutter and filter wheel, which was used to automatically shift the excitation wavelengths, the xenon lamp housing and the filter wheel assembly were coupled to the microscope with a bent optical fiber (G.W. Ellis Fiberoptic Light Scrambler, Technical Video, Woods Hole, MA). The application of the light scrambler not only helped eliminate the vibration of the stage, which could otherwise destroy a whole-cell patch, but also improved the homogeneity of illumination by the exciting light (Ellis, 1979, 1985). Furthermore, the fiber coupling permitted placement of the excitation assembly outside the Faraday cage; this significantly reduced noise pick-up by the patch clamp headstage. Also, the CCD camera was mounted on the bottom of the microscope through a hole in the stainless steel top of a vibration isolation table (Watts Fluidair, Kittery, ME); in addition to providing the most efficient light path, this configuration isolated the patch clamp system from electrical noise associated with the camera electronics. To minimize exposure time and thereby reduce the photobleaching, a 2 $\times$ 2 binning of CCD pixels was always used. The exposure time for the excitation at 440 and 530 nm was 0.7 and 1.4 s, respectively. For each cell, a pair of background images (which were adjacent to the cell but contained no cells) were taken for subtraction. For each experimental day, at least one pair of flat-field images of a dye solution in ethanol were also acquired for image processing and correction (see Loew, 1994, for details).

Image analysis was performed with software (Ratioview) developed by James Schaff at the Center for Biomedical Imaging Technology, University of Connecticut Health Center. This included the flat-field correction, subtraction of the background, masking of the contour of cell membrane, and calculation of the 440-nm/530-nm ratios for the images under the mask. The mask was constructed from one of the raw images with a combination of image-sharpening filters to accentuate the ring stain pattern defining the membrane followed by automatic feature selection (magic wand), to produce a mask that covered a uniform narrow width centered on the bright ring stain. The Ratioview software was also used to calculate the average ratio in the masked ratio images and to pseudocolor the images for display.

Patch clamp

Micropipettes were pulled from borosilicate glass capillaries using a vertical pipette puller (model 720, David Kopf Instruments, Tujunga, CA) with a patch clamp adapter (model 728). The open diameter of the pipette tip was 1–2 μm with a resistance of 2–10 MΩ. The micropipettes were filled with a solution containing (in mM) 140 potassium aspartate, 5 NaCl, and 10 HEPES (pH 7.35). Currents were recorded at room temperature using a patch clamp amplifier (Axopatch 1-D, Axon Instruments, Foster City, CA). Before making a gigaseal, the junction potential was always compensated. The whole-cell configuration of patch clamp was achieved by gentle suction under voltage clamp. During calibrations of the dye, the membrane potential was clamped to different levels ranging from $-$100 mV to $+$60 mV, and a pair of images were taken at each potential and analyzed as detailed above.

For the direct electrical determination of resting potential, a whole-cell patch was first achieved under voltage clamp and was then immediately switched to current clamp. The output signal at zero current was digitized by using the Fetchex program (Axon Instruments). An amplitude histogram was then constructed and fit to a Gaussian by using a simplex least-squares algorithm (Pstat, Axon Instruments). The resting potential was taken as the fitted mean.

RESULTS

Calibration of di-8-ANEPPS in neuroblastoma N1E-115 cells

Using the patch clamp/imaging microscope described in Materials and Methods, it was possible to obtain dual-wavelength images of single cells for which the transmembrane potential was set by a whole-cell clamp. Fig. 1 gives examples at two voltages of how the fluorescence ratio (R) was derived from a neuroblastoma N1E-115 cell. The raw images were taken at the excitation wavelengths of 440 and 530 nm, respectively, at clamped voltage levels of $-$60 and 0 mV. The pseudocolor ratio images in this figure indicated that R changed with the voltage; R averaged over the perimeter of the cell was 6.15 at 0 mV and 5.50 at $-$60 mV. All of the R values used for the calibrations and transmembrane potential measurements were based on averages under a mask defining the cell perimeter.

One prerequisite for dual-wavelength ratiometric measurement of the membrane potential is that R should have a precise and preferably linear relationship to the membrane potential. We confirmed this consistency by using the whole-cell clamp to calibrate the fluorescence ratio in 40 cells (18 undifferentiated and 22 differentiated). For each cell, a whole-cell patch was established and the transmem-

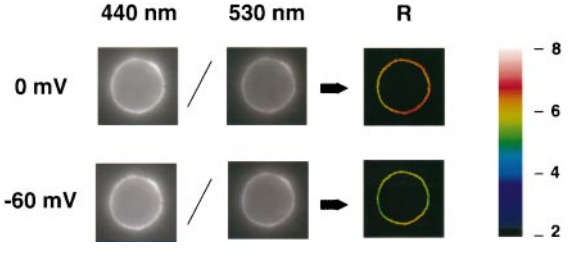

FIGURE 1 Fluorescence ratio (R) of a neuroblastoma N1E-115 cell clamped at 0 mV and $-$60 mV. This undifferentiated cell was stained with 1 μM di-8-ANEPPS and was bathed in buffered EBSS solution. The left and the middle images at each voltage were the raw images taken at the excitation wavelength of 440 nm and 530 nm, respectively. After background subtraction and flat-field correction, the pseudocolor ratio image (*right*) was obtained by dividing the 440-nm image by the 530-nm image. R was taken as the average value of the pixels corresponding to the contour of the cell membrane.

brane potential of the cell was clamped at various levels ranging from −160 mV to +60 mV. A pair of images were then taken at each voltage level, and the corresponding R value was obtained as shown in Fig. 1. In Fig. 2, we have pooled the data from these cells and plotted the normalized R against the clamped transmembrane potential. The normalized R was defined as R at a given potential divided by R at 0 mV. Normalization was used to reduce the cell-to-cell variation of R. Such variation can arise from small differences in day-to-day setup configurations of the microscope and camera system. They also can arise from the influence of membrane lipid composition on the dye fluorescence (Gross et al., 1994), which can vary with the degree of differentiation. The linear regression analysis of the data in Fig. 2 resulted in a coefficient of determination of 0.963, indicating that the regression line was able to predict the normalized R from the transmembrane potential. The slope of the regression line indicated that R changed ~15% per 100 mV transmembrane potential in these cells.

Control measurements were made to assure that light scattering from the patch pipette did not affect the fluorescence ratio measurement. For nine cells, the mean ratio was 4.16 ± 0.10 (SEM) without the pipette and 4.13 ± 0.10 after the pipette was brought into contact with the cells' membranes. Conversely, current clamp measurements were made to assure that dye staining and/or exposure to Pluronic F127 did not affect the resting potential. No significant difference between a series of controls (−30.7 ± 2.7 mV; 12 cells) and dye-stained cells (−34.5 ± 2.2 mV; 12 cells) were observed.

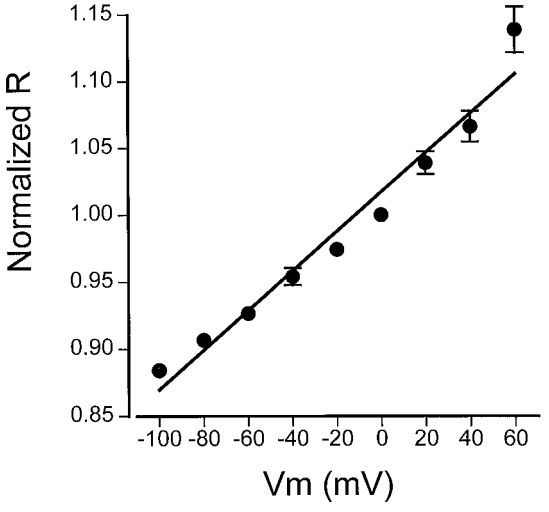

FIGURE 2 Calibration of di-8-ANEPPS in neuroblastoma N1E-115 cells. For each cell, R was normalized to the value obtained at the transmembrane potential of 0 mV. The normalized R was then plotted against the clamped transmembrane potential (V_m). The data were obtained from 40 cells, and each data point represents mean ± SEM. Not all of the cells were tested through the whole range of V_m. The calibration line was derived from linear regression of the data, resulting in a change of 0.15 of normalized R per 100 mV.

Single-cell determination of membrane potential

The resting potential of a di-8-ANEPPS-stained cell can be determined by measuring R of the cell in its resting state before establishment of the whole-cell patch. Once the cell has been patch clamped, the voltage can be varied until a value is found that produces a match with the original resting R. Fig. 3 shows how the resting potential of a single

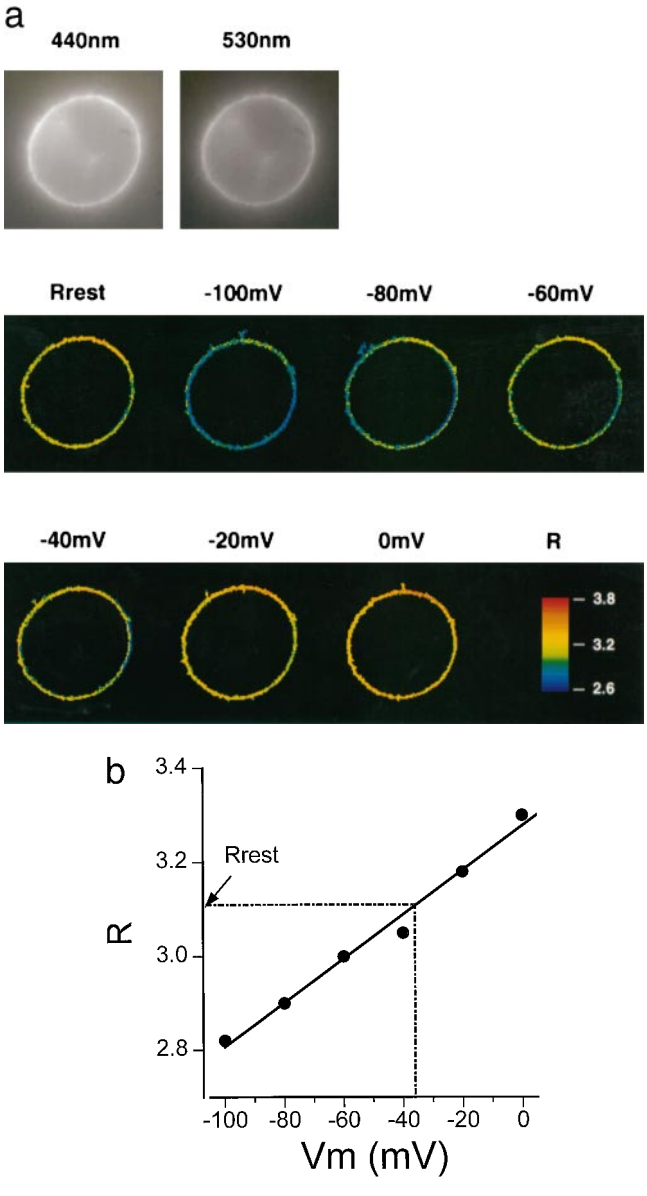

FIGURE 3 Single-cell calibration of R and measurement of resting potential. (*a*) The gray scale images were raw images taken from a resting undifferentiated neuroblastoma cell, before the establishment of a whole-cell patch. The first pseudocolor image was the corresponding ratio image (Rrest). The other pseudocolor ratio images were then obtained after establishment of the whole-cell patch when the cell membrane was clamped to different voltage levels, as indicated in the figure. (*b*) Fluorescence ratio (R) obtained in this experiment was plotted against the clamped transmembrane potential. The solid line represents a linear regression of the data, and the dotted line indicates how the resting potential of the cell was derived.

neuroblastoma N1E-115 cell was measured in practice. The cell was bathed in EBSS solution and the fluorescence ratio was obtained before introduction of the patch pipette. After establishment of the whole-cell clamp, the R values corresponding to a series of clamped transmembrane potentials were determined (Fig. 3 *a*) and fit to a calibration line by linear regression (Fig. 3 *b*). The dotted line indicates how the resting potential (which was −36 mV for this undifferentiated cell) was derived from the resting fluorescence ratio, based on the calibration line.

The variations in R along the surface of a cell are subtle, but because the images are carefully corrected for flat-field variations and the patterns are persistent at all applied voltages, we feel they are significant. In the cell of Fig. 3 *a*, for example, a persistently higher than average ratio is found in an arc centered at 1 o'clock and a low ratio arc is centered at 3 o'clock. Respectively, they correspond approximately to the equivalent of a 20-mV depolarization and a 15-mV hyperpolarization relative to the average potential. Rather than reflecting differences in transmembrane potential, these variations are likely to represent variations in dipole potential along the cell surface as has been previously found for the differentiated N1E-115 neuroblastoma cells (Bedlack et al., 1994) (see Discussion section).

Using the combined patch clamp and fluorescence ratio imaging technique, we have measured the resting potential in 13 undifferentiated cells. The mean value was -34.4 ± 3.1 mV; mean ± SEM), which was similar to that measured by using microelectrodes under similar experimental conditions. In whole-cell clamped differentiated cells, the R values were determined by averaging the perimeter of only the somata to minimize space clamp artifacts. The mean value of the resting potentials determined in these cells was -51.3 ± 3.4 mV. These results indicate that differentiation makes the resting potential significantly more negative than undifferentiated cells ($p < 0.05$ compared with the undifferentiated cells, Student's *t*-test; Fig. 4, solid bars).

The resting potential can also be estimated by whole-cell current clamp alone. We measured the resting potential in both differentiated and undifferentiated N1E-115 cells by clamping the membrane current at zero (Fig. 4, open bars).

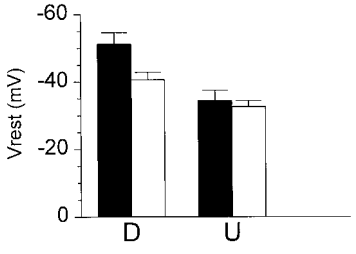

FIGURE 4 Resting potentials (Vrest) of the differentiated cells (D) and the undifferentiated cells (U) measured by combined patch clamp and fluorescence ratio imaging technique (■) and by current clamp alone (□). Error bars represent SEM. By either technique, the difference between the differentiated and undifferentiated cells was statistically significant (Student's *t*-test; $p < 0.05$).

The mean resting potential obtained from undifferentiated cells by using the current clamp alone was -32.6 ± 1.8 mV (mean ± SEM; $n = 24$). Thus, measurement of resting potential in undifferentiated cells by current clamp gives results that are similar to the fluorescence-based measurement. However, the average value of the resting potential obtained via current clamp from differentiated cells was -40.7 ± 2.2 mV (mean ± SEM; $n = 21$), which was 10.6 mV more positive than the resting potential measured by using the combined patch clamp and fluorescence ratio imaging technique (Student's *t*-test, $p < 0.05$). This discrepancy for the differentiated cells may reflect nonuniform potentials across different regions of the cell membrane or nonzero currents for the resting state of the cell.

DISCUSSION

We have shown here that the electrical properties of cell membranes, such as the transmembrane potential, can be measured by the combination of fluorescence ratio imaging and patch clamp techniques. The approach developed here combines the extraordinary precision of the patch clamp method with the ability of the fluorescent dyes to measure long-term changes in potential without seriously perturbing the intracellular milieu. Using this combined technique, we have measured the resting potentials in both differentiated and undifferentiated N1E-115 neuroblastoma cells.

Both the combined technique and the current clamp alone have shown that differentiation of these cells in low serum for 2–5 days significantly increases the absolute value of the resting potential. The N1E-115 neuroblastoma cell line has been the subject of many electrophysiological investigations, and there are several reports of resting potential measurements made with either microelectrodes or current clamp methods. For the undifferentiated cells these numbers range from −20 to −40 mV, with most reports clustered around −36 mV (Kimhi et al., 1976; Littauer et al., 1978; Milligan and Strange, 1984; Cosgrove and Cobbett, 1991; Arcangeli et al., 1995). Resting potentials for differentiated cells have been reported in the range of −35 to −66 mV (Littauer et al., 1978; Higashida et al., 1983; Tertoolen et al., 1987; Cosgrove and Cobbett, 1991). The reason for such a great spread for the values in the differentiated cells may be because of the variability in the conditions used to induce differentiation by different laboratories; a particularly careful study by Cosgrove and Cobbett (1991) showed that the resting potential measured by current clamp rose from −35 to −49 mV from 2 to 13 days of serum deprivation (without DMSO exposure). Thus, both the resting potentials of −51 mV obtained for the differentiated cells and −34 mV obtained for the undifferentiated cells by the fluorescence-based method in this study are comparable to the best of the numbers obtained by other methods.

Furthermore, whereas undifferentiated cells showed similar resting potentials measured by either the fluorescence or current clamp approaches, the differentiated cells gave sig-

nificantly more polarized potentials by the fluorescence method. (Fig. 4). The differentiated cells have long processes that may lead to nonuniform potentials in the different regions of the cell; thus, the current clamp electrode may be measuring a local potential difference across the soma membrane rather than a true resting potential. With any cell it is possible that electrogenic pumps will produce nonzero currents that might contribute significantly to the resting potential in a way that would not be measured by the current clamp method (Bashford and Pasternak, 1985). Either of these explanations could account for the discrepancy between the current clamp and fluorescence-based measurements of resting potential in the differentiated cells.

Fluorescence ratio imaging has been used to measure intracellular ionic concentrations and membrane potentials in many cell types, including neuroblastoma N1E-115 cells (Bedlack et al., 1992, 1994). The main advantage of the method is that the ratiometric measurement can cancel out some artificial variations such as uneven loading or distribution of fluorescent indicators in the cells. The dye-bleaching problem is also obviated because the resultant loss of signal would be proportional at both wavelengths. One prerequisite for correct measurements is the accurate calibration of the dyes. The voltage-sensitive dye used in the present study was previously calibrated by using the potassium/valinomycin method, in which the fluorescence ratios were calibrated against the valinomycin-mediated potassium diffusion potentials (Bedlack et al., 1992, 1994). This calibration method was sufficient for mapping spatial or temporal differences in membrane potential. However, as the intracellular potassium concentration is unknown, an accurate absolute value of the transmembrane potential cannot be derived. It was also a very delicate procedure because treatment with valinomycin can quickly cause cells to become generally permeable to ions other than K^+. Our ability to image fluorescence and, subsequently, make voltage measurements with the precision permitted by a patch clamp allowed a much more robust and precise method for calibrating R. The linear relationship between R and the transmembrane potential validated the application of this method in these cells.

The combination of these techniques offers new opportunities to study other membrane electric properties that cannot be measured by conventional micropipette alone. A significant intrinsic source of the variation in R can be the intramembrane dipole potential, which varies with the lipid composition of the cell membrane and may change with the degree of cell differentiation. Because it produces an extremely intense electrical field at the location of the dye chromophore, R is very sensitive to small variations in dipole potential (Gross et al., 1994). Indeed, the dipole potential may be an important source for the uneven distribution of electric fields along the cell surface (Figs. 1 and 3 *a*). The variations in R may relate to differences in lipid composition that could govern patterns of neurite outgrowth during differentiation. In previous studies on differentiated N1E-115 neuroblastoma cells (Bedlack et al., 1994), it was shown that the fluorescence ratio of di-8-ANEPPS was consistently higher in the neurite than in the soma, corresponding to a more negative intramembrane electric field in the latter. This was later correlated to a corresponding difference in the voltage dependent activity of sodium channels in these two regions of the cell (Zhang et al., 1996). The methods developed in this work for membrane potential imaging and patch clamp recording on the same cell should make it possible to more fully explore the dependence of channel kinetics on localized intramembrane electric fields.

We are grateful to James Schaff for providing the Ratioview Program and to Drs. Laurinda A. Jaffe, Achilles J. Pappano, and Steven J. Potashner for their helpful comments on the manuscript.

This study was supported by grant GM 35063 from the National Institutes of Health.

REFERENCES

Arcangeli, A., L. Bianchi, A. Becchetti, L. Faravelli, M. Coronnello, E. Mini, M. Olivotto, and E. Wanke. 1995. A novel inward-rectifying potassium current with a cell-cycle dependence governs the resting potential of mammalian neuroblastoma cells. *J. Physiol.* 489:455–471.

Bashford, C. L., and C. A. Pasternak. 1985. Plasma membrane potential of neutrophils generated by the Na^+ pump. *Biochim. Biophys. Acta*. 817: 174–180.

Bedlack, R. S., M.-d. Wei, S. H. Fox, E. Gross, and L. M. Loew. 1994. Distinct electric potentials in soma and neurite membranes. *Neuron*. 13:1187–1193.

Bedlack, R. S., M.-d. Wei, and L. M. Loew. 1992. Localized membrane depolarizations and localized intracellular calcium influx during electric field-guided neurite growth. *Neuron*. 9:393–403.

Cohen, L. B., and B. M. Salzberg. 1978. Optical measurement of membrane potential. *Rev. Physiol. Biochem. Pharmacol.* 83:35–88.

Cosgrove, C., and P. Cobbett. 1991. Induction of temporally dissociated morphological and physiological differentiation of N1E-115 cells. *Brain Res. Bull.* 27:53–58.

Ellis, G. W. 1979. A fiber-optic phase-randomizer for microscope illumination by laser. *J. Cell Biol.* 83:303a.

Ellis, G. W. 1985. Microscope illuminator with fiber optic source integrator. *J. Cell Biol.* 101:83a.

Grinvald, A. S., R. Hildesheim, I. C. Farber, and J. Anglister. 1982. Improved fluorescent probes for the measurement of rapid changes in membrane potential. *Biophys. J.* 39:301–308.

Gross, E., R. S. Bedlack, and L. M. Loew. 1994. Dual-wavelength ratiometric measurement of the membrane dipole potential. *Biophys. J.* 67:208–216.

Hamill, O. P., A. Marty, E. Neher, B. Sakmann, and F. J. Sigworth. 1981. Improved patch clamp techniques for high-resolution current recording from cells and cell-free membrane patches. *Pflügers Arch. Eur. J. Physiol.* 391:85–100.

Higashida, H., N. Sugimoto, K. Ozutsumi, N. Miki, and M. Matsuda. 1983. Tetanus toxin: a rapid and selective blockade of the calcium, but not sodium, component of action potentials in cultured neuroblastoma N1E-115 cells. *Brain Res.* 279:363–368.

Kimhi, Y., C. Palfrey, I. Spector, Y. Barak, and U. Littauer. 1976. Maturation of neuroblastoma cells in the presence of dimethylsulfoxide. *Proc. Natl. Acad. Sci. U.S.A.* 73:462–466.

Littauer, U. Z., C. Palfrey, Y. Kimhi, and I. Spector. 1978. Induction of differentiation in mouse neuroblastoma cells. *Natl. Cancer Inst. Monogr.* 48:333–337.

Loew, L. M. 1988. How to choose a potentiometric membrane probe. *In* Spectroscopic Membrane Probes, Vol. 2. L. M. Loew, editor. CRC Press, Boca Raton, FL. 139–152.

Loew, L. M. 1994. Voltage sensitive dyes and imaging neuronal activity. *Neuroprotocols*. 5:72–79.

Loew, L. M., S. Scully, L. Simpson, and A. S. Waggoner. 1979. Evidence for a charge-shift electrochromic mechanism in a probe of membrane potential. *Nature*. 281:497–499.

Loew, L. M., and L. Simpson. 1981. Charge shift probes of membrane potential: a probable electrochromic mechanism for ASP probes on a hemispherical lipid bilayer. *Biophys. J.* 34:353–365.

Milligan, G., and P. G. Strange. 1984. Use of [3H]triphenylmethylphosphonium cation for estimating membrane potential in neuroblastoma cells. *J. Neurochem.* 43:1515–1521.

Montana, V., D. L. Farkas, and L. M. Loew. 1989. Dual wavelength ratiometric fluorescence measurements of membrane potential. *Biochemistry*. 28:4536–4539.

Neher, E., and B. Sakmann. 1976. Single-channel currents recorded from membrane of denervated frog muscle fibers. *Nature*. 260:779–802.

Tertoolen, L., B. Tilly, R. Irvine, and W. Moolenaar. 1987. Electrophysiological responses to bradykinin and microinjected inositol polyphosphates in neuroblastoma cells. *FEBS Lett.* 214:365–369.

Tsien, R. Y., and M. Poenie. 1986. Fluorescence ratio imaging: a new window into intracellular ionic signaling. *Trends Biochem Sci.* 11: 450–455.

Waggoner, A. S. 1985. Dye probes of cell, organelle, and vesicle membrane potentials. *In* The Enzymes of Biological Membranes. A. N. Martonosi, editor. Plenum, New York. 313–331.

Zhang, J., L. M. Loew, and R. M. Davidson. 1996. Faster voltage-dependent activation of sodium channels in growth cones versus somata of neuroblastoma N1E-115 cells. *Biophys. J.* 71:2501–2508.